ISSN: 2637-6067 DOI: 10.6918/IJOSSER.202208_5(8).0100

Research on the Combustion Flame Stability of Biodiesel/Diesel Blends By Digital Image Processing Technology

Huan Mao[1,*], Zhijian Xu[1]

[1]School of Automotive and Traffic Engineering, Jiangsu University, Zhenjiang, 212013, China

[*]Email: mh1516625282@163.com

Abstract

To investigate the combustion flame stability considered one of the characteristics of combustion flame about blending biodiesel, could provide a theoretical basis for the improvement of the biodiesel combustion and the inhibition of pollutant formation. Mixed combustion with various blending ratio of biodiesel and diesel was carried out in the cylinder of diesel engine and atmospheric environment, using digital image processing technology for the pretreatment of combustion flame images acquired and the calculation and analysis of combustion flame stability from several evaluation indicators (abundance, propagation rate, circularity, height, width, effective area of flame) under two combustion environments. Then the change regularity and influence factors of flame stability were obtained, and the results revealed that in the cylinder of diesel engine, with the increase of the proportion of biodiesel blending, the flame abundance and flame propagation rate at first decreased then increased, and the flame circularity at first increased then decreased, with the increase of rotating speed, the flame propagation rate decreased, and the flame abundance and flame circularity increased obviously. In the atmospheric environment, with the increase of air flow, the height and effective area of flame at first increased and then decreased, while the flame width decreased gradually; with the increase of the proportion of biodiesel blending, the height, width and effective area of flame decreased gradually. This is mainly because the relatively high viscosity of biodiesel contributes to the worse evaporation and atomization; the decreases of oil and gas mixing uniformity and the unsteadily change of the heat from combustion and the kinetic energy of flame results in the weaker combustion flame stability. The higher rotating speed and lower air flow contribute to the increase of oil and gas mixing uniformity, the steady change of the heat from combustion and the kinetic energy of flame, which could enhance the combustion flame stability.

Keywords

Combustion flame stability; Biodiesel/diesel blends; Digital image processing; Evaluation indicators of flame stability; Diesel engine.

1. Introduction

A combustion flame can directly reflect the speed and quality of combustion. It is vital to study the combustion flame characteristics of fuel for the improvement of combustion efficiency and the reduction of pollutant emissions [1]. Therefore, combustion flame stability considered one of the flame characteristics has been investigated in this study. As an important indication of the combustion flame state, combustion flame stability plays a significant role in practical engineering applications [2].

In order to diagnose the combustion state more accurately, sets of scholars have studied the combustion flame stability of coal, H_2/CO/O_2/He, biogas, n-decane, and other fuels. Then they

ISSN: 2637-6067 DOI: 10.6918/IJOSSER.202208_5(8).0100

created numerous effective detection methods for combustion flame stability, and obtained various research results. Lu et al. [3] studied the impact of co-firing coal and biomass on flame characteristics and stability using a vision-based flame monitoring system in an on-line continuous mode. They reported that the biomass additions impact on the characteristics of the flame, particularly the flame ignition points and brightness the flame stability is little affected by the amount of biomass added provided that the addition is no more than 20%. Askari et al. [4] studied the laminar burning velocity and the flame instability of $H_2/CO/O_2$/He flames in cylindrical and spherical cavity vessels by differential multi-shell thermodynamic models. Then they analyzed flame instability on effective Lewis number, Peclet number, and flame thickness, etc. They reported that He thinner can significantly improve the flame stability because He can increase the thermal diffusivity (effective Lewis number) and the flame thickness. Hu et al. [5] experimentally studied experimentally the flame stability of biogas blended with hydrogen combustion in the constant volume combustion bomb. The experimental results show that the flame instability increases with the decrease of equivalence ratio, and the global flame stability decreases with the increase of CO_2 fractions. Chen et al. [6] investigated experimentally the influences of fuel variation and inlet air temperature on the combustion stability characteristics in a gas turbine model combustor. They found that RP-3 and n-decane exhibited similar stability behaviors. At low inlet air temperatures, when the combustor was fueled with RP-3 and n-decane, the flame was stabilized and anchored in the combustor. Bagheri et al. [7] studied the explosion limit, combustion efficiency, wall temperature, and exhaust temperature of different miniature blunt-body combustors. They concluded that the flame temperature is the highest when the equivalent ratio is 0.5, the flow rate of fuel is 10 m/s, and the wall blade is the blunt-body. Giorgi et al. [8] obtained combustion flame images using the visualization system, performed statistical and frequency analysis on the OH chemiluminescence data in the image, and used the imaging technique determining the stability factor in the flame image, performed wavelet analysis in the flame image, then studied the local instability of the flame zone to achieve the detection of combustion flame stability. Matthesa et al. [9] present an image processing-based measure for the quantitative online flame stability monitoring applicable in non-oscil-lating as well as for oscillating combustion systems. They demonstrated the applicability of the new camera-based flame stability measure with different experiments from a pilot-scale power plant using VIS as well as NIR cameras.

From the above discussions, the domestic and foreign scholars have explored the quantitative research method of the combustion flame stability and realized the effective monitoring and control for the flame stability. However, the majority of present studies are limited to the combustion flame stability of traditional fuel, the investigation for the combustion flame stability of biodiesel is rarely reported in the literature. In this study, the evaluation indicators of combustion flame stability with high generalization ability are proposed, using digital image processing technology to the calculation and analysis for the influence factors and change regularities of combustion flame stability for biodiesel–diesel blends in the cylinder environment of the diesel engine and atmospheric environment.

2. Methodology

2.1. Combustion Facility and Flame Images Acquisition

2.1.1. The Acquisition System for the Flame Images in the Cylinder of the Diesel Engine

The detailed description about the test diesel engine is from the literature [10]. The test facilities are briefly introduced in the following tables. Tab.1 shows the major technical parameters of the test diesel engine. The shooting device, AVL 513 Engine Video System high-speed camera, can quickly and repeatedly acquire the combustion flame images changing at high speed. Tab.2 shows the main technical parameters of AVL high-speed camera.

ISSN: 2637-6067 DOI: 10.6918/IJOSSER.202208_5(8).0100

Table 1. Parameters of the diesel engine

Parameters	Specifications
Model	CC490Q
Cylinder diameter /(mm)	90
Stroke /(mm)	100
Rated power /(kW)	39.7
Rated speed /(r/min)	2200
Maximum torque /(N·m)	152
Maximum torque speed /(r/min)	1500

Table 2. Main technical parameters of AVL high-speed camera

Parameters	Specifications
Maximum exposure rate /(time/s)	60000
Endoscope diameter /(mm)	4
Image resolution /(ppi)	640×480
Dynamic range /(bit)	12
Minimum exposure time /(ms)	10
Synchronization	Crank angle
Flash time /(ms)	30
Storage capacity /(piece)	30000

Figure 1 shows the acquisition combustion flame images in the cylinder of the diesel engine as B0 is burning at a load of 0 and a speed of 1500 r/min.

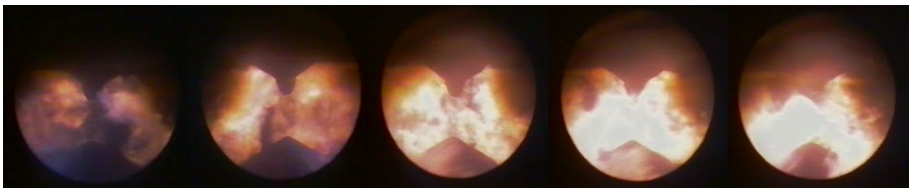

(a) -2.7°CA (b) -2.2°CA (c) 0.4°CA (d) 4.5°CA (e) 7.5°CA

(f) 11°CA (g) 12.8°CA (h) 15.8°CA (i) 19.3°CA (j) 22°CA

(k) 25.2°CA (l) 29.2°CA (m) 33.9°CA (n) 35.8°CA (o) 41.4°CA

Figure 1. Combustion flame images in cylinder of diesel engine

2.1.2. The Acquisition System for the Flame Images in the Atmosphere

The combustion test facilities for the experiment in the atmosphere primarily contains a trace oil pump, burner, air flow meter, and air pump, etc. Figure 2 (a) and Figure 2 (b) show the layout

ISSN: 2637-6067 DOI: 10.6918/IJOSSER.202208_5(8).0100

diagram and system structure diagram, respectively. The corresponding parameters of the trace oil pump and burner are shown in Table 3 and Table 4, respectively. The test fuel is 0# diesel (China National Petroleum Corporation) and soybean biodiesel whose corresponding parameters are shown in Table 5. The high-speed camera (Canon F0816) is used to acquire the combustion flame images for a different proportion of biodiesel (B0, B25, B50, B75 and B100, the figure represents the volume ratio of biodiesel to diesel) in five different air volume flow rates (0 L/min, 3 L/min, 6 L/min, 9 L/min and 12 L/min). The fuel temperature is 25 ℃ and the fuel is supplied with the volume flow rate of 0.8 mL/min.

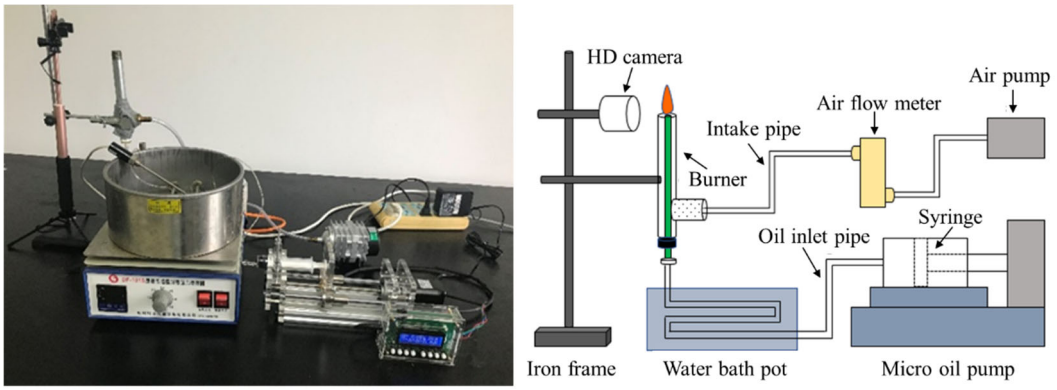

(a) Layout diagram of combustion test system (b) Structure diagram of combustion test system

Figure 2. Layout diagram and structure diagram of combustion test system

Table 3. Main performance parameters of micro-oil pump

Parameters	Specifications
Type	Clamping table
Speed range	0.01mm/s~0.21mm/s (mL/s), 0.01mm/min~12.50mm/min (mL/min), 0.01mm/h~99.99mm/h (mL/h)
Time setting / (s / min / h)	1s~17h
Way of working	Manual control, timing work, communication control
Slider stroke / (mm)	140
Single turn lead / (mm)	1
Size / (mm)	290×130×130
Working power / (V / A)	12/2
Adapter power supply / (V / Hz)	100~240/50

Table 4. Relevant dimension parameters of the burner

Parameters	Specifications
Quartz tube inner diameter / (mm)	5
Quartz tube outer diameter / (mm)	7
Double-pass stainless steel tube inner diameter / (mm)	20
Double-pass stainless steel tube outer diameter / (mm)	23
Plug thickness / (mm)	12

ISSN: 2637-6067 DOI: 10.6918/IJOSSER.202208_5(8).0100

Table 5. Comparison of physicochemical characteristics between soybean biodiesel and diesel fuel

Physical and chemical properties	0# diesel	Soybean biodiesel
Calorific value / (MJ·kg^{-1})	42.5	37.5
Density (20 °C) / (g·mL $^{-1}$)	0.837	0.885
Oxygen content / (%)	0	10.89
Kinematic viscosity (20 °C) / (mm^2·s^{-1})	3.2	4.5
Flash point / (K)	328	>422
Cetane number	45	47.1
Sulfur content / (μL·L^{-1})	196	<3

Figure 3 shows the combustion flame images in the atmosphere at different fuel mixture ratios (B0, B25, B50, B75, and B100) with a fuel temperature of 25 °C and an air flow rate of 0 L/min.

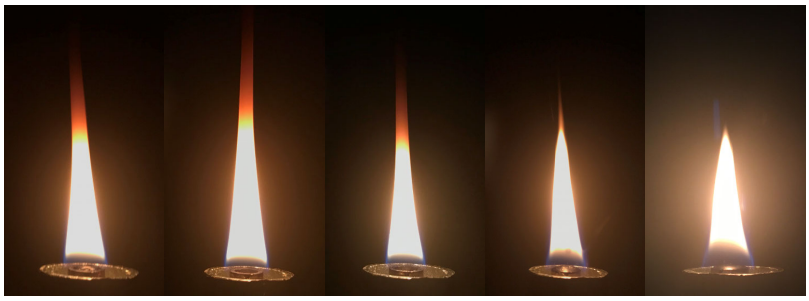

(a) B0 (b) B25 (c) B50 (d) B75 (e) B100

Figure 3. Combustion flame images in the atmospheric environment

2.2. The Processing Method of Flame Images

There are some problems such as noise interference, low contrast, and fuzzy edge structure [11] on the flame images obtained by the image acquisition system, which is not conducive to the extraction of the flame characteristic parameters such as flame abundance, flame effective area, etc. Thus, it is very necessary to process flame images to improve the calculation accuracy via the digital image processing technology. The main process of the digital image processing technology contains image denoising and image segmentation. In this study, the median filtering method is adopted to remove noise from flame images [11]. For image segmentation, Otsu method is adopted due to its stable performance and strong adaptability [12].

Fig.4 shows the original image, gray image, denoising image, and segmentation image of the flame from left to right. For the segmentation image, the white area represents the flame area and its edge represents the edge of the flame area, and the black indicates the background color. The flame and background are separated and the flame edge outline is clear through image segmentation, which facilitates the calculation for the flame characteristic parameters.

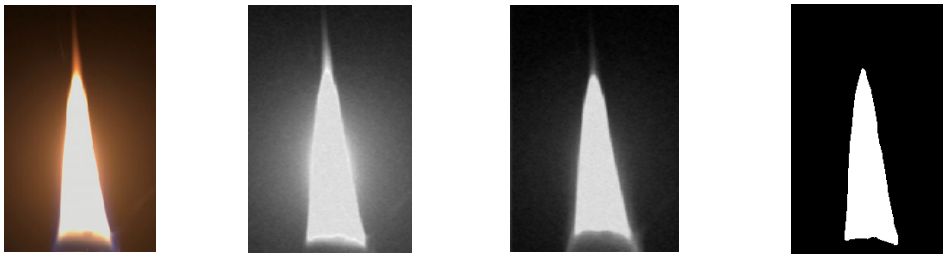

(a) Original flame image (b) Gray image (c) image denoising (d) image segmentation

Figure 4. Image denoising and segmentation of original flame image

ISSN: 2637-6067 DOI: 10.6918/IJOSSER.202208_5(8).0100

2.3. Evaluation Indicators and Calculation Schemes for Flame Stability

2.3.1. Flame Abundance

Flame abundance refers to the proportion of flame filled with the whole combustion chamber in the combustion process, that is, the proportion of flame area on the obtained image to the combustion chamber area on the whole image. In general, the more stable the flame propagation, the greater its abundance [13]. For the flame images of mixed fuel with different blending ratios at different rotating speeds in the diesel engine cylinder, flame abundance (F_f) is calculated using MATLAB with pixel area method. The flame abundance expressed in the following equation (1).

$$F_f = \frac{S_1}{S_2} \tag{1}$$

Where S_1 is the effective area of the flame and S_2 is the area of the total image (cm^2).

2.3.2. Flame Propagation Rate

During the combustion in the diesel engine cylinder, due to the constant turbulence intensity and other factors, the front surface of the flame is constantly wrinkled and broken, which makes the flame surface increase gradually, further increases the contact area between the flame surface and the unburned mixture, intensifies the self-acceleration phenomenon of flame propagation and increases the flame propagation rate (V_f). It can be seen that the larger flame propagation rate reflects that the flame area fluctuates greatly and the flame stability weakens at the corner of the adjacent crankshaft. In this paper, the flame propagation rate is defined as the change rate of flame effective area per unit crankshaft rotation angle, and it expressed in the following equation.

$$V_f = \left| \frac{S_{\varphi_2} - S_{\varphi_1}}{\varphi_2 - \varphi_1} \right| \tag{2}$$

Where V_f is the flame propagation rate($cm^2 \cdot °CA^{-1}$), φ_1 and φ_2 are diesel engine crankshaft angle, $S_{\varphi 1}$ and $S_{\varphi 2}$ are the effective area of flame for φ_1 and φ_2. The calculated flame propagation rate V_f is the propagation rate at the rotation angle of φ_1 and φ_2 median crankshafts.

2.3.3. Flame Circularity

As an important geometric feature of the flame image, circularity (C_l) can reflect flame stability accurately [13]. The circularity, the degree of similarity with the circle, represents the similarity between the outer outline of the measured flame image and the standard circle in this paper. It is usually defined as the ratio of the circumference of the circle equal to the flame area to the perimeter of the outer outline of the flame during calculating the circularity of the flame image. If the combustion state is stable and the flame shape is relatively regular, the flame shape is full and the circularity is larger. On the contrary, if the combustion state is unstable, the flame shape is disorderly and the circularity is relatively small. Flame circularity expressed in the following equations.

$$C_1 = \frac{\pi D}{L} \tag{3}$$

ISSN: 2637-6067 DOI: 10.6918/IJOSSER.202208_5(8).0100

$$D = 2\sqrt{\frac{S}{\pi}} \tag{4}$$

Where, D is the diameter (mm) of the circle equal to the flame area, L is the perimeter of flame profile (mm), S is the area (cm^2) of the effective area of the flame image.

2.3.4. Height and Width of Flame

The flame height (H) is defined as the height from the center of the nozzle plane to the top corner of the flame, and the flame width (W) is defined as the maximum width of the flame diffusion zone at the nozzle of the burner. When the height and width of the flame are larger, the stability of the flame is stronger. In this paper, the characteristic size of the flame is measured by the characteristic size proportion. The flame image size (H_1, W_1) in Fig.5 could be easily obtained according to the pixel point, the actual size is obtained according to formulas (5) and (6), respectively.

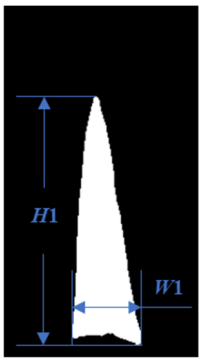

Figure 5. Related dimension marking

$$H = \alpha \cdot H_1 \tag{5}$$

$$W = \alpha \cdot W_1 \tag{6}$$

Where α is the ratio which is calculated by the ratio of the actual burner size to the image size.

2.3.5. Effective Area of Flame

The effective area of flame (S) is the effective area obtained by dividing the combustion flame with the gray threshold. Under different air flow rates, the larger the effective area of the combustion flame is, the stronger flame stability is stronger, and vice versa. The effective area of flame expressed in the following equation (7).

$$S_h = \frac{6.4516 N_2}{N_1} \tag{7}$$

Where N_1 is the number of pixels in the effective region of the flame, and N_2 is the number of pixels in the high-temperature region of the flame.

ISSN: 2637-6067 DOI: 10.6918/IJOSSER.202208_5(8).0100

3. Research Results and Discussion

3.1. Combustion Flame Stability in the Cylinder of Diesel Engine

3.1.1. Flame Abundance

Fig.6 shows the variation of flame abundance with different fuel mixture ratios (B0, B50, and B100) under the condition of 1500 r/min and 2200r/min. It can be seen that the flame abundance increases at first and then decreases with the increase of the crankshaft rotation angle. The maximum value is obtained at about 5 °CA, and the flame abundance decreases at first and then increases with the increase of the biodiesel blending ratio. From this perspective, it could be seen that the combustion flame stability of B0, B50 and B100 is B0 > B100 > B50. Because the flame gradually sweeps through the whole combustion chamber after the fuel in the cylinder is compressed and caught fire, but with the continuous increase of the crankshaft angle, the fuel is consumed and the flame extension range is gradually reduced until it is extinguished. The heat released from the combustion process decreases, the intensity of flame development decreases, and the flame abundance decreases gradually as the blending ratio of biodiesel increases from B0 to B50 [14]. This can be attributed to the slightly lower calorific value of biodiesel than diesel and the less heat released by unit mass fuel combustion. However, biodiesel contains about 11% oxygen, which can visibly promote the combustion process in the cylinder and make up for the energy loss caused by the slightly lower calorific value [15]. In a word, the flame abundance increases gradually when the blending ratio of biodiesel continues to increase from B50 to B100.

It can also be seen from Fig.6 that with the increase of rotating speed, the peak value of flame abundance increases visibly, and the average fluctuation amplitude decreases in the working cycle. At 1500 r/min speed, the peak values of combustion flame abundance of B0, B50 and B100 were 0.75, 0.58 and 0.68, respectively, and the average fluctuation amplitudes were 0.15, 0.14 and 0.21, respectively. At 2200 r/min speed, the peak values of flame abundance of B0, B50 and B100 were 0.97, 0.84 and 0.92, respectively, and the average fluctuation amplitudes were 0.13, 0.12 and 0.18, respectively, compared with the former, the flame abundance growth rates were 29.3%, 44.8%, and 35.3%, respectively. Therefore, the stability of flame propagation in the cylinder increases obviously at a higher speed. This_result may be explained by the fact that the increase of rotating speed contributes to the intensification of turbulent motion in the cylinder which results in the more uniform mixing of oil and gas, then the combustion is promoted [16].

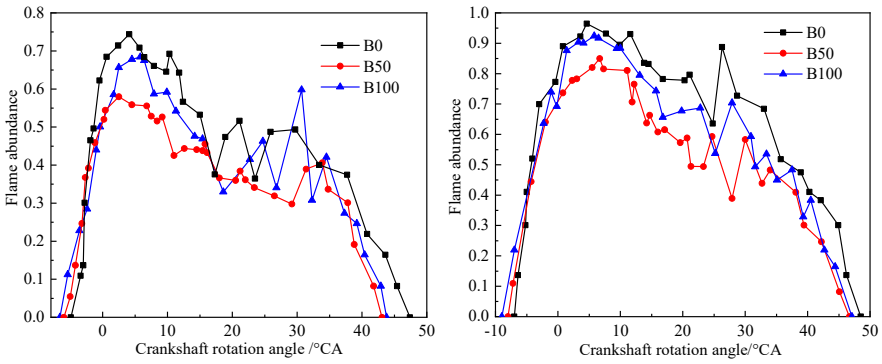

(a)1500 r/min (b)2200 r/min

Figure 6. Flame abundance

3.1.2. Flame Propagation Rate

Figure 7 shows the variation of flame propagation different fuel premixed ratios (B0, B50, and B100) under the condition of 1500 r/min. It can be seen that with the increase of crankshaft

ISSN: 2637-6067 DOI: 10.6918/IJOSSER.202208_5(8).0100

rotation angle, the flame propagation velocity increases at first and then decreases, and then tends to fluctuate smoothly, in sum, the change of flame area increases at first and then decreases gradually. This result may be explained by the fact that in the range of -4 °CA to 1 °CA, the temperature of the mixed gas increases rapidly, the flame spreads rapidly, and the change rate of flame area increases gradually. After 1 °CA, the fuel consumption is further consumed, the combustion rate decreases, the flame changes from filling the whole combustion chamber to gradually extinguishing, the flame area change speed slows down gradually, which makes the flame propagation rate decrease gradually and the flame development tend to be stable in the cylinder.

Figure 7 shows that in the range of -4 °CA to 1 °CA, with the increase of biodiesel blending ratio, the flame propagation rate decreases gradually, and the stability of B100 combustion flame is the most stable, and after 1 °CA, with the increase of biodiesel blending ratio, the flame propagation rate increases gradually, and the combustion flame of B0 is the most stable. Since in the range of -4 °CA to 1 °CA, the calorific value of diesel is slightly higher than biodiesel, and the heat released during combustion is more than biodiesel, and the viscosity of diesel is smaller and the atomization effect is slightly better than biodiesel, which makes the combustion reaction more intense and the change rate of the flame area is larger [17]. After 1 °CA, the change of flame area for biodiesel is more obvious than diesel due to the high viscosity of biodiesel, the continuous combustion of macromolecular oil droplets, and the underburned over-concentrated mixture area. At this time, with the increase of the biodiesel blending ratio, the change rate of the flame area increases gradually, and the stability of flame propagation decreases gradually.

Combined with the variation of flame propagation rate at two rotating speeds in Fig.7, it can be seen that with the increase of rotating speed, the flame propagation rate decreases, the amplitude of flame fluctuation decreases gradually, and the flame stability increases. At 1500 r/min speed, the peak values of flame propagation rates of B50 and B100 are 8.83 $cm^2 \cdot °CA^{-1}$, 6.69 $cm^2 \cdot °CA^{-1}$ and 5.61 $cm^2 \cdot °CA^{-1}$, respectively. At 2200 r/min speed, the peaks of flame propagation rates of B50 and B100 are 7.04 $cm^2 \cdot °CA^{-1}$, 4.75 $cm^2 \cdot °CA^{-1}$ and 3.73 $cm^2 \cdot °CA^{-1}$, respectively, which are 20.3%, 29% and 33.5%, respectively. The increase of intake volume contributes to the increase of turbulence in the cylinder, the rapid propagation of flame, and the decrease of flame area change rate, that is, the decrease of flame propagation rate and the enhancement of flame stability [18].

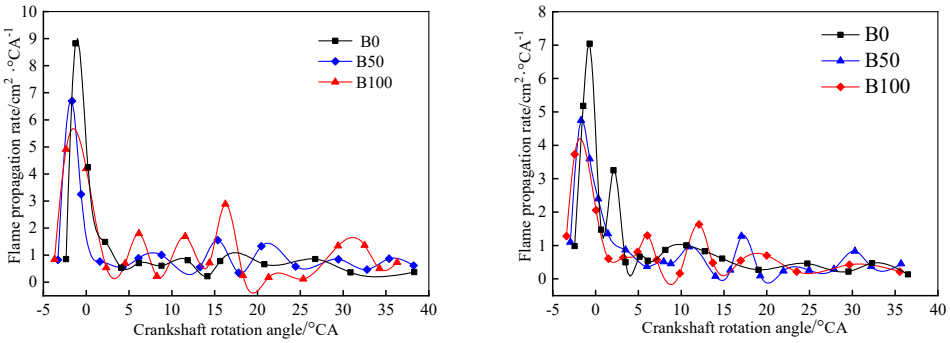

(a)1500 r/min (b)2200 r/min

Figure 7. Flame propagation rate

3.1.3. Flame Circularity

Fig.8 shows the variation of flame propagation rate of B0, B50, and B100 under the condition of 1500 r/min. It can be seen that with the increase of the crankshaft rotation angle, the flame circularity increases at first and then decreases gradually. This result may be explained by the fact that with the flame filling the whole combustion chamber rapidly in the cylinder after

ISSN: 2637-6067 DOI: 10.6918/IJOSSER.202208_5(8).0100

ignition, the flame shape is full, and the ratio of edge circumference to area increases gradually, which makes the flame circularity increase gradually. With the continuous combustion, the mixture is further consumed, the combustion intensity decreases gradually, the flame front separation intensifies, the ratio of perimeter to area decreases gradually, and the circularity decreases gradually.

Simultaneously, it can be seen from Fig.8 that before 15 °CA, the circularity of fuel combustion flame with various blending ratios has little difference. After 15 °CA, the flame circularity increases at first and then decreases with the increase of the biodiesel blending ratio. In the whole combustion cycle, the flame circularity of B50 is the largest, the numerical fluctuation is the smallest, and the flame propagation stability is the strongest, while the circularity of B100 is the smallest, the numerical fluctuation is the largest, and the flame propagation stability is the weakest. This is because the oxygen in biodiesel promotes the continuous combustion reaction and makes the combustion more fully, and compared with the flame under B0 condition, the combustion flame shape of B50 is fuller, the circularity is larger, the flame development is more stable. When the blending ratio of biodiesel continues to increase to B100, the calorific value of the mixed fuel will decrease visibly, which will reduce the heat released by the combustion [19], and the ratio of flame perimeter to area will decrease gradually. Therefore, the circularity of the B100 combustion flame is small and the flame stability is weak.

Besides, it can be seen from Fig.8 that the circularity of flame also increases, and the flame stability is further strengthened with the increase of rotating speed. At 1500 r/min speed, the peak value of flame circularity is about 0.75. At 2200 r/min speed, the peak value of flame circularity is about 0.78, which is 4% higher than that of the former. This result may be explained by the fact that as the rotating speed of the engine increases, the air movement in the cylinder is strengthened and the quality of the mixture is improved, which makes the flame morphology and structure full [20], the ratio of edge perimeter to area increases visibly, the flame circularity increases, and the flame propagation stability increases.

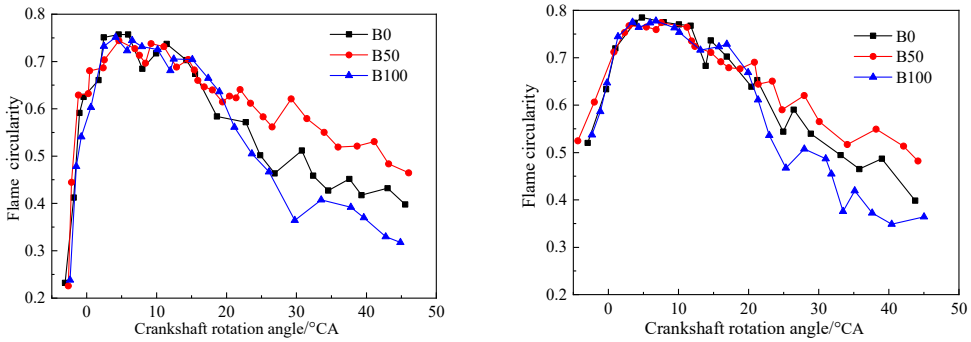

(a)1500 r/min (b)2200 r/min

Figure 8. Flame circularity

3.2. Combustion Flame Stability in the Atmosphere

3.2.1. Height and Width of Flame

Fig.9 shows the variation of flame height and width with air flow rate of mixed fuels with different blending ratios. It can be seen that with the increase of air flow rate, the flame height increases at first and then decreases, and the flame width decreases gradually. Among them, B0, B25, B50, B75, and B100 flame have the maximum flame height at the air flow rate of 3 L/min, which are 37.6 mm,33.7 mm,31.3 mm,30.3 mm and 28.5 mm, respectively, that is, the flame is the most stable when the air flow rate is 3 L/min. This is mainly since under the condition of low air flow rate, the mixing of oil and gas is more uniform, and the oxygen in the mixture is further supplemented, which promotes the combustion, increases the pressure difference

ISSN: 2637-6067 DOI: 10.6918/IJOSSER.202208_5(8).0100

between the flame and the outside world, increases the uplift buoyancy, and increases the flame height. The large air flow rate will reduce the mixing time of fuel and gas, reduce the amount of mixture, decrease the uniformity, and reduce the intensity of combustion.

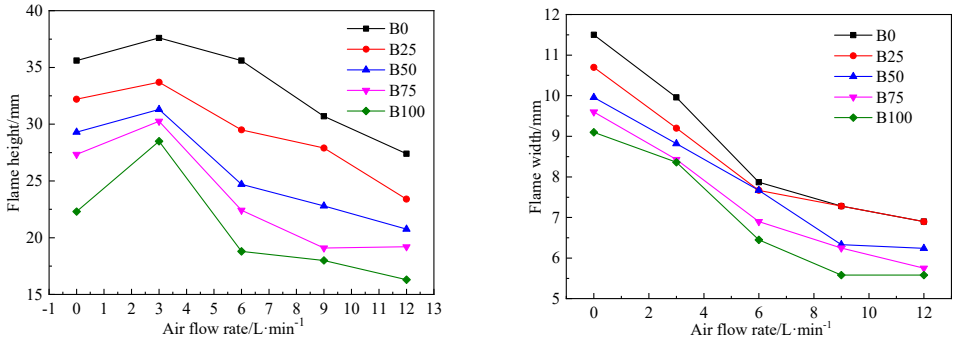

(a)Flame height (b)Flame width

Figure 9. Height and width of flame

Meanwhile, with the increase of the blending ratio of biodiesel, the height and width of flame decrease gradually, the fluctuation phenomenon of the two increases gradually, and the flame stability decreases gradually. It can be seen that the flame is the most stable as B0 is burning, and the weakest as B100 is burning. This can be attributed to the slightly lower calorific value of biodiesel and the less heat released from the combustion, which makes the pressure difference between the flame and the outside world decrease, and the flame height and width decrease [21].

3.2.2. Effective Area of Flame

Figure 10 shows the variation of the effective area of the flame of the mixed fuel with the air flow rate in different blending ratios. It can be seen that, with the increase of air flow, the effective area of the flame is increased, and the combustion flame of B0, B25, B50, B75, and B100 all obtain the maximum of the effective area of the flame when the air flow rate is 3 L/ min and is 14.3 cm^2, 13.2 cm^2, 12.3 cm^2, 11.7 cm^2, and 10.5 cm^2, respectively. The flame the most stable at the air flow rate of 3 L/ min. Since the lower air flow, the oxygen in the mixture is supplemented, the combustion is promoted, the ability of the flame to diffuse to the outside is gradually enhanced, and the effective area of the flame is gradually increased [22]. When the air flow is too large, the air flow with a too strong flame edge will take part of the mixed gas, so that the mixing time of the oil and gas is reduced, and the normal combustion of the mixed gas is not favorable. The effective area of the flame is gradually reduced when the blending ratio of the biodiesel is increased. In which, as B0 is used, the effective area change range of the flame is the smallest, the stability is the most. As the B100 is used, the change amplitude of the effective area of the flame is the largest and the stability is the weakest. This result may be explained by the fact that the lower heat value of the biodiesel causes the reduction of heat released by the combustion, the higher viscosity of the biodiesel is unfavorable to the heating and evaporation of the fuel, the uniformity of the mixture is reduced, the heat released by the combustion is also reduced, and the ability of the flame to extend outward is reduced, resulting in a reduction of the effective area of the flame [23].

ISSN: 2637-6067 DOI: 10.6918/IJOSSER.202208_5(8).0100

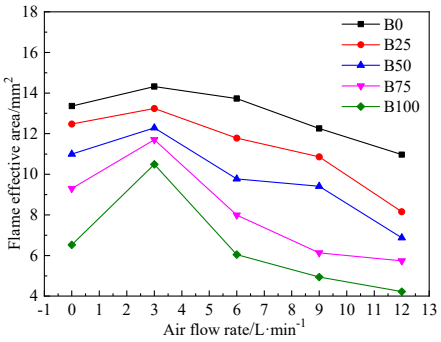

Figure 10. Flame effective area

4. Conclusions

In this paper, the combustion flame stability in the cylinder of diesel engine and the atmosphere was studied by digital image processing technology for the pretreatment of combustion flame images acquired and the calculation and analysis of combustion flame stability from six evaluation indicators. The effects of mixing ratio, rotating speed and air flow were analyzed on combustion flame stability. Conclusions could be found as following:

(1) In the cylinder of the diesel engine, the flame abundance increases at first and then decreases with the increase of crankshaft angle, the flame abundance increases at first and then decreases with the increase of biodiesel blending ratio, the peak value of flame abundance increases obviously with the increase of rotating speed. Within the range of -4°CA to 1°CA, the flame propagation rate decreases gradually with the increase of the proportion of biodiesel blending. Simultaneously, the combustion flame of B100 is the most stable. After 1°CA, with the increase of the proportion of biodiesel blending, the flame propagation rate increases gradually, and the combustion flame of B0 is the most stable. With the increase of rotating speed, the flame propagation rate and its fluctuation amplitude decrease gradually, but the combustion flame stability increases. Before 15°CA, there is little difference for the flame circularity of fuel combustion with different blending ratios. After 15°CA, the flame circularity at first increases and then decreases with the increase of biodiesel blending ratio; the circularity of flame also increases with the increase of rotating speed.

(2) In the atmosphere, with the increase of air flow, the flame height and effective area first increase then decrease, and the flame width decreases gradually. The maximum height and effective area are obtained at the air flow rate of 3 L/min for B0, B25, B50, B75, and B100. The maximum flame height was 37.6 mm, 33.7 mm, 31.3 mm, 30.3 mm, and 28.5 mm, respectively. The maximum flame effective area was 14.3 cm^2, 13.2 cm^2, 12.3 cm^2, 11.7 cm^2 and 10.5 cm^2, respectively. With the increase of the proportion of biodiesel blending, the height, width, and effective area of flame gradually decrease, and the flame stability gradually weakens. The flame stability is the most stable as B0 is burning, and the combustion flame stability is the weakest as B100 is burning.

References

[1] Zhou C, Wang Y, Jin Q, Chen Q, Zhou Y. Mechanism analysis on the pulverized coal combustion flame stability and NOx emission in a swirl burner with deep air staging[J]. Journal of the Energy Institute, 2019, 92(2): 298-310.

[2] Oishi Y, Situmorang RS, Sembiring RA, Kawai H, Ambarita H. Performance, rate of heat release, and combustion stability of dual-fuel mode in a small diesel engine[J]. Energy Science & Engineering, 2019, 7(4):1333-1351.

ISSN: 2637-6067 DOI: 10.6918/IJOSSER.202208_5(8).0100

[3] Lu G, Yan Y, Cornwell S, Whitehouse M, Riley G. Impact of co-firing coal and biomass on flame characteristics and stability[J]. Fuel, 2008, 87(7):1133-1140.

[4] Metghalchi H, Wang Z, Sirio M, Vien K, Askari O. On the flame stability and laminar burning speeds of syngas/O2/He premixed flame[J]. Fuel, 2017, 190(Feb.15): 90-103.

[5] Hu Z, Zhang X. Experimental study on flame stability of biogas/hydrogen combustion[J]. International Journal of Hydrogen Energy, 2019, 44(11): 5607-5614.

[6] Chen F, Ruan C, Yu T, Cai W, Mao Y, Lu X. Effects of fuel variation and inlet air temperature on combustion stability in a gas turbine model combustor[J]. Aerospace Science and Technology, 2019, 92: 126-138.

[7] Bagheri G, Hosseini SE, Wahid MA. Effects of bluff body shape on the flame stability in premixed micro-combustion of hydrogen–air mixture[J]. Applied Thermal Engineering, 2014, 67(1-2): 266-272.

[8] Sciolti A, De Giorgi MG, Campilongo S, Ficarella A. Image processing for the characterization of flame stability in a non-premixed liquid fuel burner near lean blowout[J]. Aerospace science and technology, 2016, 49(Feb.): 41-51.

[9] Matthes J, Waibel P, Vogelbacher M, Gehrmann HJ, Keller HB. A new camera-based method for measuring the flame stability of non-oscillating and oscillating combustions[J]. Experimental Thermal and Fluid Science, 2019,105: 27-34.

[10] Mao GP, Wang Z, et al. Effect of Biodiesel Combustion Flame Temperature on NOx Formation in Diesel Engine[J]. Chinese Internal Combustion Engine Engineering, 2011, 32(3): 1-5.

[11] Wang Q, Ma J, Yu S, Tan L. Noise detection and image denoising based on fractional calculus[J]. Chaos, Solitons & Fractals, 131, 109463.

[12] Xiao L, Ouyang H, Fan C. An improved Otsu method for threshold segmentation based on set mapping and trapezoid region intercept histogram[J]. Optik, 2019, 196: 163106.

[13] Dong ZS, Liu MJ. Flame image intelligent diagnosis method for high temperature and low oxygen[M]. Beijing: Publishing House of Electronics Industry, 2012.

[14] Zhang D, Cao D, He G, Liu B, Qin F. Investigation on combustion mode and heat release in a model scramjet engine affected by shocks[J]. International Journal of Hydrogen Energy, 2019, 44(52): 28330-28341.

[15] Seraç MR, Aydm S, Yılmaz A, Şevik S. Evaluation of comparative combustion, performance, and emission of soybean-based alternative biodiesel fuel blends in a CI engine[J]. Renewable Energy, 2020, 148: 1065-1073.

[16] Gehmlich RK, Mueller CJ, Ruth DJ, Nilsen CW, Skeen SA, Manin J. Using ducted fuel injection to attenuate or prevent soot formation in mixing-controlled combustion strategies for engine applications[J]. Applied Energy, 2018, 226: 1169-1186.

[17] Calder J, Roy MM, Wang W. Performance and emissions of a diesel engine fueled by biodiesel-diesel blends with recycled expanded polystyrene and fuel stabilizing additive[J]. Energy, 2018, 149: 204-212.

[18] DuttaRoy R, Chakravarthy SR, Sen AK. Experimental investigation of flame propagation and stabilization in a meso-combustor with sudden expansion[J]. Experimental Thermal and Fluid Science 2018, 90: 299-309.

[19] Trevor Seidel GK, Wayne S. Seames. Characterizing flame stability and radiative heat transfer in non-swirling oxy-coal flames using different multiphase modeling frameworks[J]. Fuel, 2019, 256, 115948.

ISSN: 2637-6067 DOI: 10.6918/IJOSSER.202208_5(8).0100

[20] Luo Q-h, Sun B-g. Experiments on the effect of engine speed, load, equivalence ratio, spark timing and coolant temperature on the energy balance of a turbocharged hydrogen engine[J]. Energy Conversion and Management, 2018, 162: 1-12.

[21] Medhat Elkelawya HA-EB, Khaled Khodary Esmaeila, et al. Experimental studies on the biodiesel production parameters optimization of sunflower and soybean oil mixture and DI engine combustion, performance,and emission analysis fueled with diesel/biodiesel blends[J]. Fuel, 2019, 255, 115791.

[22] Zhang B, Liu Z, Li W, Luan B, He J, Dong J. Characteristic visualization of the micro/mesoscale liquid ethanol diffusion flame by using deflection tomography[J]. International Communications in Heat and Mass Transfer, 2018, 96: 43-52.

[23] Kumar S, Dinesha P, Rosen MA. Effect of injection pressure on the combustion, performance and emission characteristics of a biodiesel engine with cerium oxide nanoparticle additive[J]. Energy, 2019, 185: 1163-1173.